Clusters of II−VI Materials: Cd_iX_i, X = S, Se, Te, $i \leq 16$

Jon M. Matxain,* Jose M. Mercero, Joseph E. Fowler, and Jesus M. Ugalde

Kimika Fakultatea, Euskal Herriko Unibertsitatea, P.K. 1072, 20080 Donostia, Euskadi, Spain

Received: October 22, 2003; In Final Form: August 30, 2004

Several structures of small Cd_iX_i clusters, $i \leq 16$, have been characterized. Ringlike structures have been found to be the lowest lying structures for $i \leq 5$ clusters and three-dimensional spheroid structures for larger ones, $i = 6-16$. This trend has been ascribed to the stability of obtuse X−Cd−X angles in the first case and to the stability gained from higher coordination in the second case. The three-dimensional structures may be envisioned as being built from Cd_2X_2 squares and Cd_3X_3 hexagons, as it was the case for Zn_iO_i, X = O, S, Se, Te, and Cd_iO_i three-dimensional structures, studied previously in our group. Second-order free-energy differences reveal that the most stable spheroids are the $i = 12$ ones. The highest occupied molecular orbital−lowest unoccupied molecular orbital gaps are found to fit in the experimental trend observed for nanoparticles, which might be an indication of a possible reorganization of the nanoparticle surfaces. Vibrational spectra are provided for their use in experimental characterization.

1. Introduction

Semiconductors are materials of great importance in the development of technology. Computer revolution and other technological devices are in rapid development basically because of improved semiconductor materials. Some of these materials are the II−VI compounds, in which interest has increased notably because of their paramount technological potential. Applications such as photovoltaic solar cells,[1−10] optical sensitizers,[11] photocatalysts,[12,13] or quantum devices[14] have led to extensive investigation of their properties. To understand them it is essential to study the structure and electronic properties of these compounds, thereby providing more information for the rational design of these materials to enhance their applicability. Many theoretical studies have been reported concerning the bulk electronic structure of these compound semiconductors.[15−22] Studies on their clusters are more scarce.

There are properties of these compounds that have been seen to be local phenomena. That is, when they happen, they happen at a certain well-defined domain. Consequently, the study of small clusters of these compounds could give insight into these local properties, including their catalytic behavior.[23] Also, the fact that cluster and nanoparticle characterization is becoming technologically feasible is remarkable. This makes cluster science even more interesting, because in addition to its capability in helping rationalize some of their surface-related properties, studies of clusters of increasingly larger size can eventually fill the gap with the nanosize materials domain in a comprehensible manner.[24] For instance, in studying clusters of silicon of increasing size, it has be found that the driven force for the stability of Si nanoparticles of diameter $d < 5$ nm (up to 2500 Si atoms) is the surface energy minimization. This renders icosahedral lowest energy structures that deviate markedly form the bulklike structure. The latter is often assumed to be the preferred one until the cluster approaches the limit of a few hundred atoms. However, it has been shown[25] that when the bulk has a tetrahedrally coordinated structure, like Si and the materials of the present investigation, there is no a priori reason to assume a bulklike structure for the nanoparticles. As a matter of fact, experimental studies on nanoparticles of 2−6 nm in diameter are becoming routine work.[26,27] The case of II−VI nanoparticles is not an exception. Binary compounds such as ZnO[28,29] and ZnS,[30,31] CdS,[32−37] CdSe,[37−42] and CdTe[37,43,44] and ternary compounds such as CdS/ZnS,[45] CdSe/ZnSe,[46,47] CdTe/ZnTe,[48] and CdSe/CdTe[49] have recently been studied. These nanoparticles are grown in solution, where organic molecules surround the nanoparticle to stop its growth. It is assumed that the structure of these particles is a bulklike core surrounded by a reconstructed surface. The nature of this surface reconstruction is not known, but its properties are determinant in the chemistry of these nanoparticles. This growth of experimental works has led to an increased interest of complementary theoretical works on II−VI clusters.[50−52]

Theoretical calculations have previously been performed in our group for Zn_iX_i, $i = 1-9$, X = O, S, Se, Te, clusters[53−55] and Cd_iO_i, $i = 1-9$, 12, 15, clusters.[56] In ref 57 we predicted the existence of fullerene-like spheroids of Zn_iO_i. Recently, experimentally synthesized[58] Zn_iO_i clusters, $i = 9$, 11, 15, have been related to the spheroid structures predicted theoretically, which could be the confirmation of the existence of this type of structure. In this paper we focus on Cd_iX_i, $i \leq 16$, X = S, Se, Te, clusters. We have been able to characterize spheroid structures with diameters of 0.96, 0.99, and 1.06 nm for Cd_iS_i, Cd_iSe_i, and Cd_iTe_i, respectively, which lie close to the experimentally smallest detected II−VI nanoparticles, namely, 1.8 and 3 nm in diameter for CdSe and CdTe, respectively. This means that available theoretical and experimental data on small nanoparticles are actually merging.

2. Method

Characterized structures have been found by using local minimization procedures. The starting structures were chosen according to previous studies of other II−VI clusters and chemical intuition. All the tried structures converged to the ones presented in this study or to some others that are not presented because they are very high in energy. Some bulklike structures were attempted but converged to spheroids.

All geometries were fully optimized using the hybrid[59] Becke 3 Lee−Yang−Parr (B3) gradient-corrected approximate density-

10.1021/jp037195s CCC: $27.50
Published on Web 10/29/2004

TABLE 1: SKBJ(d/2df) and SKBJ(expan) Exponents for Cd, S, Se, and Te Atoms[a]

	SKBJ(d/2df)				SKBJ(expan)			
	Cd α	S α	Se α	Te α	Cd α	S α	Se α	Te α
sp					0.261 148	1.231 541	0.750 763	0.535 452
sp					0.182 01	0.373 393	0.375 285	0.180 824
d	0.23	0.7	0.537 83	0.349 496	1.350 188	0.896 605	0.691 855	0.408 953
d			0.208 111	0.155 952	0.23	0.288 732	0.463 247	0.237 585
d					0.097 397		0.177 490	0.084 947
f			0.396 026	0.306 353	1.451	0.593 345	1.048 712	0.594 100
f					0.326 695		0.366 780	0.228 881

[a] All the coefficients are 1.

TABLE 2: Cd−X Bond Lengths and X−Cd−X and Cd−X−Cd Angles of Ring Structures

	R (Cd−X)			α (X−Cd−X)			α (Cd−X−Cd)		
	X = S	X = Se	X = Te	X = S	X = Se	X = Te	X = S	X = Se	X = Te
$^{(1)}Cd_2X_2^{R(I)}$	2.49	2.60	2.79	110.8	113.2	116.9	69.2	66.8	63.1
$^{(1)}Cd_2X_2^{R(II)}$	2.59	2.68	2.87						
$Cd_3X_3^{R(I)}$	2.42	2.52	2.72	155.9	159.1	161.5	84.1	81.6	78.5
$Cd_3X_3^{R(II)}$	2.42−2.48	2.53−2.57	2.53−2.57	126.6−135.2	132.1−140.3	132.1−140.3			
$Cd_4X_4^R$	2.39	2.50	2.70	176.0	178.1	177.7	93.9	91.5	87.3
$Cd_5X_5^R$	2.38	2.49−2.50	2.69−2.70	175.1−177.9	173.4−179.1	171.9−178.3	97.8	94.5	90.5
$Cd_6X_6^R$	2.38	2.49	2.70	178.0	178.2	178.4	99.2	95.0	90.5
$Cd_7X_7^R$	2.38	2.49	2.70	174.9−178.9	174.6−179.0	174.6−178.4	99.6−101.2	94.7−97.0	89.6−92.0
$Cd_8X_8^R$	2.38	2.49	2.70	178.3	177.8	177.5	99.9	95.5	90.9
$Cd_9X_9^R$	2.38	2.49	2.70	174.7−179.2	175.4−179.5	176.5−179.6	99.9−100.6	95.0−96.1	90.3−91.4
$Cd_{10}X_{10}^R$	2.38	2.49	2.70	177.8	177.6	177.6	100.5	95.7	90.9
$Cd_{11}X_{11}^R$	2.38	2.49	2.70	173.0−179.5			100.0−101.6		
$Cd_{12}X_{12}^R$	2.38	2.49	2.70	178.0	177.3−179.3	177.9−179.7	100.6	95.6	90.8

functional procedure.[60−62] Harmonic vibrational frequencies were determined by analytical differentiation of gradients.

The relativistic compact effective core potentials and shared-exponent basis set[63] of Stevens, Krauss, Basch, and Jasien (SKBJ) were used as the basic basis set in this study. The 4d electrons of Cd were included in the valence. To perform the geometry optimizations and harmonic frequency calculations an extra d functions set was added on Cd and on S, and two additional d and one f set for Se and Te, due to their importance for the proper description of the high coordination of the atoms in the three-dimensional cluster structures. This basis set is denoted as SKBJ(d/2df), and the exponents are shown in Table 1. However, the energy calculations were performed with an even more expanded basis set, denoted as SKBJ(expan), to obtain accurate relative energies. The exponents of all of these added functions were energy optimized using the GAMESS[64] package. Note that pure angular momentum functions were used throughout this study.

All the geometry optimizations and frequency calculations were carried out with the Gaussian 98[65] package.

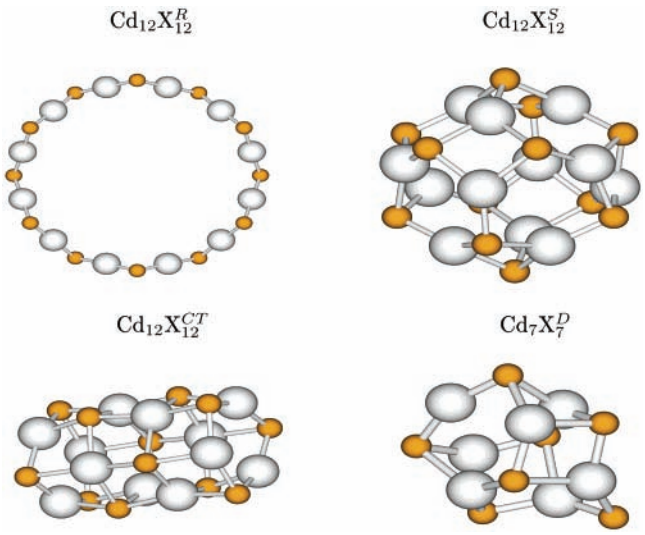

Figure 1. Structures of each cluster family of Cd_iX_i. Dark smaller atoms are those of X.

3. Results

3.1. Structures of Characterized Minima of Cd_iX_i, X = S, Se, Te, $i \leq 16$. In this section the calculated structures are described. Different types of families have been characterized, which are rings (R), chains (C), spheroids (S), distorted spheroids (D), and cluster tubes (CT). The difference between spheroids and distorted spheroids will be made clear below. Structures are labeled according to the following scheme: $^{(s)}Cd_iX_i^a$, where (*s*) denotes the multiplicity and *i* the number of CdX units and the superscript *a* stands for the structure family. A representative structure of each family is shown in Figure 1. Molecular geometries such as the bond length and bond angles are given in Tables 2 (rings), 3 (spheroids), and 4 (chains, distorted spheroids, and cluster tubes). Note that triplet states have been considered only for small clusters, $i = 1, 2$, because they stand high in energy for larger clusters. Hence, for $i \geq 3$ spin multiplicity will not be shown. X may be S, Se, or Te. Hereafter, when using Cd_iX_i, it will be to all Cd_iS_i, Cd_iSe_i, and Cd_iTe_i that we will be referring.

Rings are planar for small clusters ($i \leq 5$ for Cd_iS_i, $i \leq 4$ for Cd_iSe_i and Cd_iTe_i) and near planar for larger ones. The main reason to break the planarity in these ring structures is the observed strong tendency to form linear X−Cd−X angles and Cd−X−Cd angles between 100 and 90°. Thus, the X−Cd−X bond angles lie within 170−180° for these rings, and Cd−X−

TABLE 3: Cd−X Bond Lengths and X−Cd−X Angles of Spheroids

	R (Cd−X)			α (X−Cd−X)		
	X = S	X = Se	X = Te	X = S	X = Se	X = Te
$Cd_4X_4^S$	2.61	2.72	2.90	103.0	104.8	107.1
$Cd_6X_6^S$	2.50−2.75	2.62−2.84	2.82−3.02	98.3−143.3	100.3−143.8	102.7−143.3
$Cd_8X_8^S$	2.49−2.68	2.60−2.79	2.81−2.97	96.9−138.8	98.6−140.2	101.0−140.2
$Cd_9X_9^S$	2.49−2.62	2.60−2.73	2.80−2.92	97.5−132.7	99.6−140.9	101.3−140.7
$Cd_{10}X_{10}^S$	2.47−2.63	2.58−2.75	2.78−2.93	95.3−137.8	96.8−139.8	98.6−139.7
$Cd_{11}X_{11}^S$	2.48−2.63	2.58−2.74	2.79−2.93	91.7−138.3	92.4−140.3	94.5−140.3
$Cd_{12}X_{12}^S$	2.47−2.58	2.58−2.69	2.79−2.88	94.5−131.1	95.8−131.3	98.0−130.7
$Cd_{13}X_{13}^S$	2.48−2.64	2.59−2.75	2.78−2.93	93.0−137.8	93.8−139.6	95.3−139.7
$Cd_{14}X_{14}^S$	2.47−2.61	2.58−2.71	2.78−2.94	92.1−136.4	93.4−138.3	95.6−138.1
$Cd_{15}X_{15}^S$	2.47−2.58	2.58−2.69	2.78−2.88	94.5−132.3	95.9−132.6	98.0−132.3
$Cd_{16}X_{16}^S$	2.51−2.55	2.62−2.66	2.82−2.86	94.6−131.7	95.9−131.7	97.5−131.1

TABLE 4: Cd−X Bond Lengths and X−Cd−X Angles of Chains, Distorted Spheroids, and Cluster Tubes

	R (Cd−X)			α (X−Cd−X)		
	X = S	X = Se	X = Te	X = S	X = Se	X = Te
$Cd_1X_1^C$	2.29	2.40	2.61			
$^{(3)}Cd_2X_2^C$	2.31−2.44	2.42−2.56	2.62−2.79	177.8	177.5	177.5
$Cd_5X_5^D$	2.37−2.64	2.48−2.75	2.60−2.74	98.3−152.4	97.1−154.8	97.1−154.8
$Cd_7X_7^{D(I)}$	2.38−2.65	2.49−2.75	2.69−3.13	94.2−177.3	96.5−176.3	98.9−177.8
$Cd_7X_7^{D(II)}$	2.43−2.82	2.48−2.90	2.68−3.07	91.3−154.9	92.6−157.7	95.1−138.6
$Cd_8X_8^{CT}$	2.49−2.69	2.59−2.91	2.80−3.05	94.3−155.3	98.0−160.4	101.2−155.8
$Cd_9X_9^{CT}$	2.50−2.74	2.61−2.89	2.79−3.17	92.4−168.4	93.0−149.6	93.5−159.0
$Cd_{12}X_{12}^{CT}$	2.50−2.75	2.60−2.89	2.80−3.32	92.1−164.9	84.6−159.4	90.0−154.8
$Cd_{15}X_{15}^{CT}$	2.50−2.75	2.60−2.91	2.80−3.27	93.3−165.3	92.1−160.4	91.2−156.4

Cd tend to 100° for CdS, to 95° for CdSe, and to 90° for CdTe. The bond lengths decrease as the size of the ring increases from 2.54 to 2.38 Å for Cd_iS_i, 2.66 to 2.49 Å for Cd_iSe_i, and 2.89 to 2.69 Å for Cd_iTe_i. Spheroids can be depicted as being built from $Cd_2X_2^R$ (squares)- and $Cd_3X_3^R$ (hexagons)-like structures. The number of squares remains constant, six, while the number of hexagons increases by one when adding a new CdX unit. A similar structural tendency is observed in Zn_iX_i clusters.[53−55,57] In fullerenes there are pentagons instead of squares, but similarly the number of pentagons remains constant, 12, and the number of hexagons increases by one adding two carbon atoms. Spheroids that do not follow this trend are labeled as distorted spheroids. $Cd_7X_7^{D(II)}$ and $Cd_5X_5^D$ are built by squares and hexagons, while $Cd_7X_7^{D(I)}$ has also octagons. Finally, cluster tubes are built by rings located parallel to each other, forming short tubes. All these structures have been described in detail elsewhere.[56]

In Figure 2 the relative energies for all shown Cd_iX_i clusters are plotted versus the number of CdX units, *i*. In the region of small clusters, $i \leq 5$, rings are found to be the most stable structures. Chains are stable only for small sizes, $i = 1, 2$. Spheroids become more stable as the cluster size increases, and as it can be observed in the region of $6 \leq i \leq 16$, they are the most stable structures. In the case of $i = 7$ distorted spheroids are the most stable ones, but while for Cd_iS_i and Cd_iSe_i $Cd_7X_7^{D(I)}$ is the most stable one, for Cd_iTe_i this structure lies above the other distorted spheroid, $Cd_7X_7^{D(II)}$. Results for $i \leq 7$ are in agreement with previous theoretical calculations. Finally, we observe that, as the cluster size increases, the relative energy between spheroids and rings and cluster tubes increases, the spheroids being the dominant ones. Although similar plots are obtained for all Cd_iX_i, the most salient feature is that as X goes down in the periodic table from S to Te, the relative energies decrease as well. This is consistent with the relative energies found for Cd_iO_i clusters[56] and Zn_iX_i, X = O, S, Se, Te, clusters.[53−55] This trend may be seen clearly in Figure 3, where the relative energies between rings and three-dimensional structures are shown for all Zn_iX_i and Cd_iX_i combinations. These relative energies are calculated as $\Delta E = E_{3D} - E_{ring}$. Thus, when ΔE is positive, the ring structure is more stable and so on. When both the Cd_iX_i and the Zn_iX_i series are compared, it is observed that the relative energies are very similar for both cases, which means that Zn and Cd have similar behavior at least in these compounds, and the differences come mainly from X atoms. The main difference is that ring structures are more stable than spheroids for $i \leq 7$, in the case of Zn_iO_i and Cd_iO_i, while for $i \leq 5$ in the case of the remaining combinations. This may be explained by the larger ability of S, Se, and Te to achieve higher coordination, due to the d orbitals which, however, are very high in energy for O. The break of ring planarity occurs at different cluster sizes for different compounds, that is, $i = 4$ for Y_iSe_i and Y_iTe_i (Y = Zn, Cd), $i = 5$ for Y_iS_i and Cd_iO_i, and $i = 7$ for Zn_iO_i. In these compounds the break of planarity occurs at a smaller size as X goes down in the periodic table. In other words, the larger the size of X, the more difficult it is to achieve linear angles. The larger size of Cd with respect to Zn explains why for CdO rings the break occurs at a smaller size compared to ZnO clusters.

3.2. Stability. Cohesive Energies and Second-Order Free-Energy Differences. It has been demonstrated elsewhere[66] that many cluster properties, in accordance with the liquid drop model, lie within lines when plotted versus $i^{-1/3}$, where *i* is the number of CdX units. The cohesive energy

$$E_f = \frac{iE_{Cd} + iE_X - E_{Cd_iX_i}}{i} \quad (1)$$

is one of these properties. It has been observed both theoretically and experimentally for Si_i clusters[67] that clusters belonging to the same family lie within a line. The family lying above is the

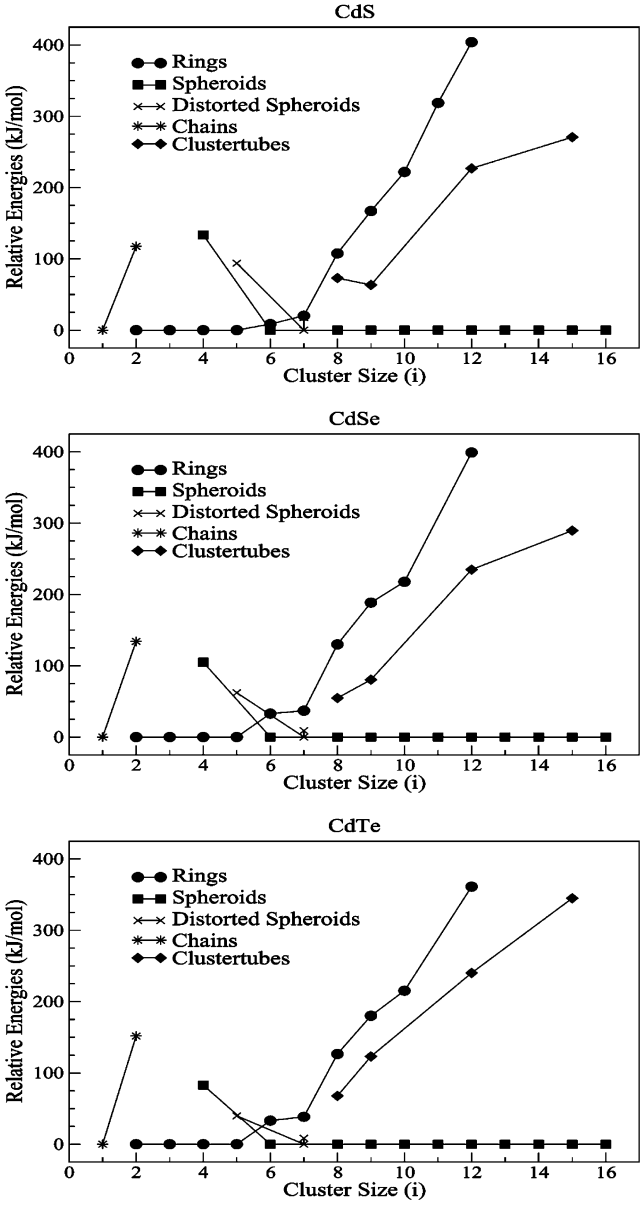

Figure 2. Relative energies for Cd_iX_i clusters: starting from above, Cd_iS_i, Cd_iSe_i, and Cd_iTe_i clusters, respectively.

most stable family in that cluster size range. The cohesive energies of the three families of Cd_iX_i clusters, $i = 3-15$, X = S, Se, Te, namely, rings, spheroids, and cluster tubes, are plotted versu $i^{-1/3}$ in Figure 4.

The points corresponding to the ring structures lie on a line with smaller slope than that of the spheroids and cluster tubes. For small clusters the ring line lies above that of the spheroids and cluster tubes. But at $i = 6$ there is a crossing and the spheroids lie above, while the cluster tubes lie between the spheroids and the rings. Qualitatively all three graphs are similar, though the cohesive energies are found to decrease as X goes down in the periodic table, which is consistent with experimental data.

Fitting a line to the spheroid points and extrapolating it to $i^{-1/3} = 0$, the theoretical value for the cohesive energy of a hypothetical infinite-size spheroid can be obtained. The predicted cohesive energies are 469.62, 432.24, and 363.79 kJ/mol for CdS, CdSe, and CdTe, respectively. In the infinite-size region the bulk is the most stable structure. The bulk cohesive energies are calculated by eq 2,

$$E_{f,exp} = |\Delta H_f^\circ(CdX) - \Delta H_f^\circ(Cd) - \Delta H_f^\circ(X)| - RT \quad (2)$$

and according to the CODATA data[68] are 550.09 and 401.0 kJ/mol for CdS and CdTe, respectively. No experimental data for CdSe have been found.

The cohesive energy is an estimator of the stability; the larger the cohesive energy, the more stable the structure is. The spheroid's extrapolated cohesive energies are close to the bulk ones, which indicates that the stability of the spheroids is large in this size region, $i = 6-16$. This statement has been confirmed for ZnO clusters, as we predicted, in ref 58 by Bulgakov et al.

The second free-energy difference is a measurement of the stability of the structures. It is also often used as a measure of local stability. We will use it as a measurement of the stability of spheroids. It can be calculated according to

$$\Delta_2 G(Cd_iX_i^S) = G(Cd_{i+1}X_{i+1}^S) + G(Cd_{i-1}X_{i-1}^S) - 2G(Cd_iX_i^S) \quad (3)$$

and positive values of it correspond to stable structures. These stable structures are associated with electronic shell closure within the jellium model.[69] Gibbs free energies have been used in the calculation of the second differences. The graphs of $\Delta_2 G$ shown in Figure 5 display maxima at $i = 6$, 9, 12, and 15. The peak corresponding to $i = 12$ is clearly the most positive one. This suggests that the $Cd_{12}X_{12}$ spheroids are the most stable of the studied spheroids. In Figure 6 we provide the vibrational spectra of these most stable spheroids, to help in the characterization of these species.

3.3. Highest Occupied Molecular Orbital−Lowest Unoccopied Molecular Orbital (HL) Gaps and Experimental Absorption Energies. HL gaps may be used as an estimator of the excitation energies. They are an upper bound to the true excitation energy,[57] and as the particle size increases the gap approaches the true excitation energy. We have calculated these

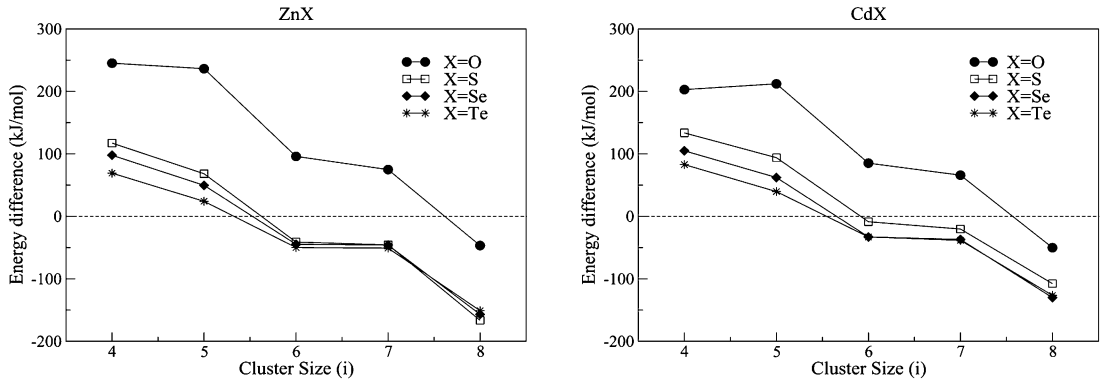

Figure 3. Relative energies for Y_iX_i clusters: Zn_iX_i on the left and Cd_iX_i on the right.

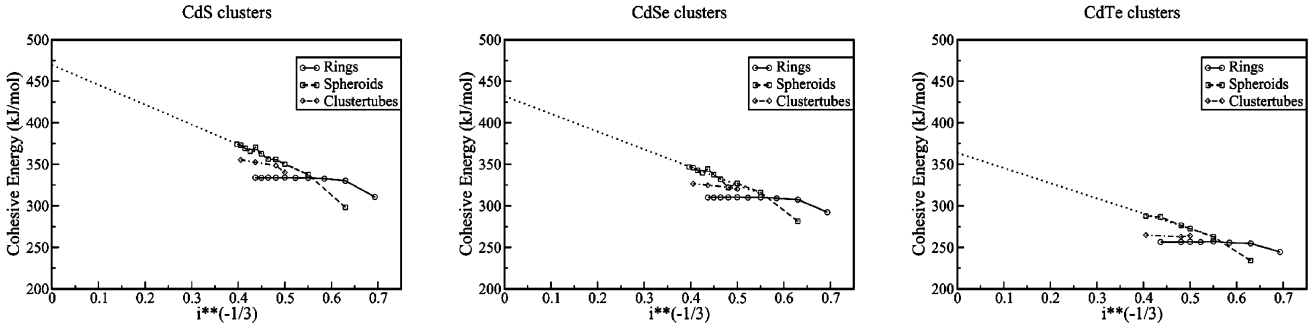

Figure 4. Cohesive energies of Cd_iX_i clusters: starting from the left Cd_iS_i, Cd_iSe_i, and Cd_iTe_i clusters, respectively.

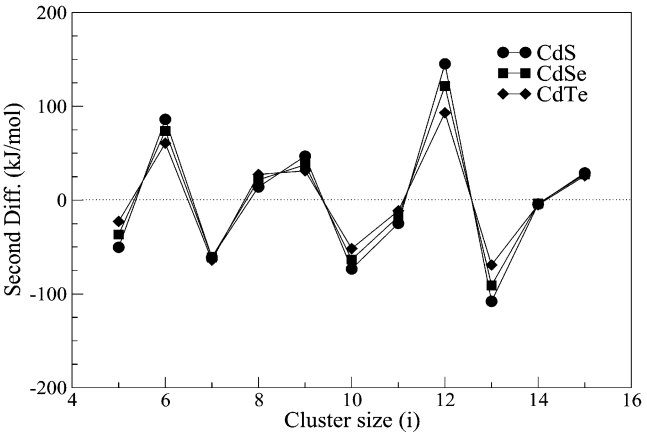

Figure 5. Second differences in energy calculated using Gibbs free energies.

gaps for the characterized spheroids, rings, and cluster tubes, and they are depicted versus the diameter of the particle in Figure 7. For all CdX the largest HL gaps correspond to rings, and the smallest ones correspond to cluster tubes. The experimentally grown nanoparticles are assumed to be spherical with a bulklike crystal structure at the core and a reconstructed surface.[70,71] The shape of this surface reconstruction is not well-known yet. It is also assumed that the number of atoms of the core are much larger than those of the surface. As the particle size increases, the absorption energy decreases toward bulklike values. This can be observed in Figure 7 as well, where the values of absorption energies tend to bulk values, namely, 2.42 eV for CdS, 1.74 eV for CdSe, and 1.45 eV for CdTe.[1] Comparing HL gaps of clusters with experimental data of smallest nanoparticles, we observe that the HL gaps of spheroids do follow the nanoparticle trend. In the case of the smallest nanoparticles, the importance of the surface absorption is much larger than in large nanoparticles, where the surface/volume ratio is much larger. That is, the absorption energies in the smallest nanoparticles occur mainly in the surface. The similarity between the spheroid's HL gaps and the absorption energies of nanoparticles could be due to structural similarities between them; that is, the nanostructure surface resembles the square−hexagon structure of spheroids. Nevertheless, excitation energies should be calculated to confirm these similarities.

Another point of interest is the fact that when the nanocrystal structures become more stable than spheroids. Experimental nanoparticles are grown in solution, while our calculations are in the gas phase, which makes it difficult to obtain a strong conclusion, but with the data available some predictions can be made. Recall that the coordination number of spheroids is

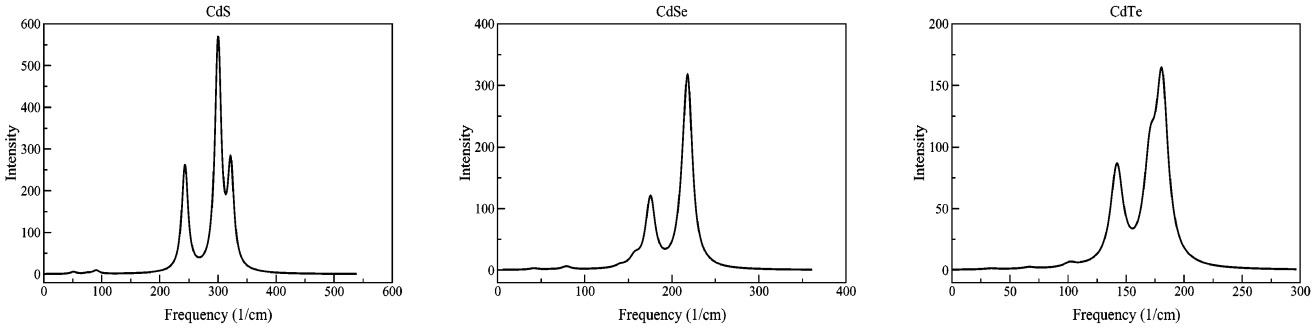

Figure 6. Vibrational spectra for the most stable spheroids, $Cd_{12}X_{12}$.

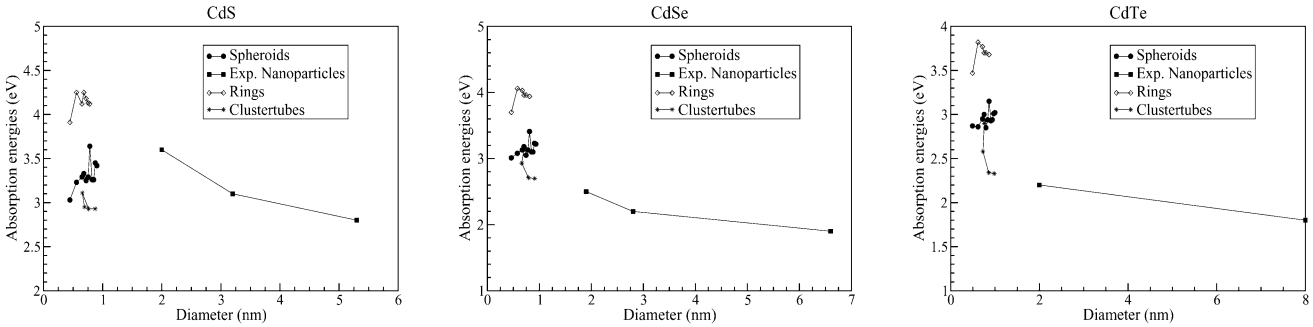

Figure 7. HL gaps of spheroid, ring, and cluster tube structures and absorption energies of experimental nanoparticles. CdS values taken from ref 39, CdSe values from ref 40, and CdTe values from ref 41.

three while that of the bulk is four. In solution, the atoms of the nanoparticle placed in the surface can achieve the fourth coordination number in the interaction with solvent molecules, which can favor bulklike nanocrystals against spheroids. We, therefore, think that spheroids could be difficult to obtain in the experiments that are carried out in solution. However, for experiments made in the gas phase, these spheroids could be characterized. These experiments have been carried out for ZnO, and spheroids have been found, as we predicted.[57]

4. Conclusions

Several structure families of the clusters Cd_iX_i, $i = 1-16$, X = S, Se, Te, have been studied. They are found to undergo a ring-to-three-dimensional structural transition. This behavior parallels that of the previously investigated Zn_iX_i clusters, X = S, Se, Te, but differs markly from that of Zn_iO_i and Cd_iO_i clusters. This is due to the fact that oxygen d orbitals lie higher in energy and the ability of S, Se, and Te to achieve higher coordination is larger. The structural transition alluded to above arises from a delicate balance between two opposite tendencies. On one hand, rings are favored by the tendency to linearity of the X−Cd−X bonds, and on the other hand, three-dimensional structures are favored by the tendency to achieve higher coordination. Our calculations indicate that the former dominates when the higher coordination does not carry too much strain for the bond angles. This takes place at $i = 8$ for Cd_iO_i and Zn_iO_i and at $i = 6$ for Zn_iX_i, Cd_iX_i, X = S, Se, Te. Naturally, the smaller size of the oxygen valence orbitals accounts for its transition occurring at higher cluster sizes.

The predicted structures of the lowest energy three-dimensional spheroid structures of Cd_iX_i can be envisioned as being built of smaller basic building units, namely, the Cd_2X_2 squares and Cd_3X_3 hexagons. These structures appear to be the basic structural units for larger clusters in the same sense that C_5 pentagons and C_6 hexagons constitute the basic structural units of fullerenes. Second-order differences in energy points out that the most stable spheroids in all cases are $Cd_{12}X_{12}$. The transition to cluster structures having a larger coordination number, or bulklike structure, is predicted to happen for cluster size $i > 16$. The diameter of these spheroids is roughly half that of the smallest nanoparticles found experimentally. The experimental nanoparticles are assumed to have bulklike structures; however, a reorganization of the surface on these structures is seen to happen. According to the HL differences of spheroids and absorption energies of nanoparticles, these surface reconstructions could happen in a way where the surfaces resemble a spheroid. We think that these spheroids could be found in gas-phase experiments, as has recently been the case of several small Zn_iO_i spheroids, predicted previously by our group.

Acknowledgment. This research was funded by Euskal Herriko Unibertsitatea (The University of the Basque Country), Eusko Jaurlaritza (the Basque Government), and the Ministerio de Educacion y Ciencia.

References and Notes

(1) Chu, T. L.; Chu, S. S. *Solid-State Electron.* **1995**, *38*, 533.
(2) Halliday, D. P.; Eggleston, J. M.; Durose, K. *Thin Solid Films* **1998**, *322*, 314.
(3) Yamamoto, T.; Toyama T.; Okamoto, H. *Jpn. J. Appl. Phys.* **1998**, *37*, L916.
(4) Lee, J. H.; Lee, H. Y.; Park, Y. K.; Shin, S. H.; Park, K. J. *Jpn. J. Appl. Phys.* **1998**, *37*, 3357.
(5) Singh, V. P.; McClure, J. C.; Lush, G. B.; Wang, W.; Wang, X.; Thompson G. W.; Clark, E. *Sol. Energy Mater. Sol. Cells* **1999**, *59*, 145.
(6) Burgelman, M.; Nollet P.; Degrave, S. *Appl. Phys. A* **1999**, *69*, 149.
(7) Durose, K.; Edwards, P. R.; Halliday, D. P. *J. Cryst. Growth* **1999**, *197*, 733.
(8) Contreras, G.; Vigil, O.; Ortega, M.; Morales, A.; Vidal, J.; Albor, M. L. *Thin Solid Films* **2000**, *361−362*, 378.
(9) Chakrabarti, R.; Dutta, J.; Bandyopadhyay, S.; Bhattacharyya, D.; Chaudhuri, S.; Pal, A. K. *Sol. Energy Mater. Sol. Cells* **2000**, *61*, 113.
(10) Edwards, P. R.; Galloway, S. A.; Durose, K. *Thin Solid Films* **2000**, *361−362*, 364.
(11) Sebastian, P. J.; Ocampo, M. *Sol. Energy Mater. Sol. Cells* **1996**, *44*, 1.
(12) Hoffman, A. J.; Mills, G.; Yee, H.; Hoffmann, M. R. *J. Phys. Chem.* **1992**, *96*, 5546.
(13) Kuwabata, S.; Nishida, K.; Tsuda, R.; Inoue, H.; Yoneyama, H. *J. Electrochem. Soc.* **1994**, *141*, 1498.
(14) Corcoran, E. *Sci. Am.* **1990**, *263*, 74.
(15) Schroer, P.; Kruger, P.; Pollmann, J. *Phys. Rev. B* **1993**, *47*, 6971.
(16) Schroer, P.; Kruger, P.; Pollmann, J. *Phys. Rev. B* **1993**, *48*, 18264.
(17) Schroer, P.; Kruger, P.; Pollmann, J. *Phys. Rev. B* **1994**, *49*, 17092.
(18) Vogel, D.; Kruger, P.; Pollmann, J. *Phys. Rev. B* **1995**, *52*, 14316.
(19) Pollmann, J.; Kruger, P.; Rohlfing, M.; Sabisch, M.; Vogel, D. *Appl. Surf. Sci.* **1996**, *104/105*, 1.
(20) Vogel, D.; Kruger, P.; Pollmann, J. *Phys. Rev. B* **1996**, *54*, 5495.
(21) Muilu, J.; Pakkanen, T. A. *Surf. Sci.* **1996**, *364*, 439.
(22) Muilu, J.; Pakkanen, T. A. *Phys. Rev. B* **1994**, *49*, 11185.
(23) Shou-heng, S.; Chuan, S.; Fink, K.; Staemmler, V. *Chem. Phys.* **2003**, *287*, 183.
(24) Castleman, A. W.; Bowen, K. H. *J. Phys. Chem.* **1996**, *100*, 12911.
(25) Zhao, Y.; Kim, Y.; Du, M.; Zhang, S. B. *Phys. Rev. Lett.* **200**4, *93*, 015502.
(26) van der Boom, T.; Hayes, R. T.; Zhao, Y.; Bushard, P. J.; Weiss, E. A.; Wasielewski, M. R. *J. Am. Chem. Soc.* **2002**, *124*, 9582.
(27) Wang, Y. A.; Li, J. J.; Chen, H.; Peng, X. *J. Am. Chem. Soc.* **200**2, *124*, 2293.
(28) Tokumoto, M. S.; Pulcinelli, S. H.; Santilli, C. V.; Briois, V. *J. Phys. Chem. B* **2003**, *107*, 568.
(29) Pesika, N. S.; Hu, Z.; Stebe K. J.; Searson, P. C. *J. Phys. Chem. B* **2002**, *106*, 6985.
(30) Denzler, D.; Olschewski, M.; Sattler, K. *J. Appl. Phys.* **1998**, *84*, 2841.
(31) Calandra, P.; Longo, A.; Liveri, V. T. *J. Phys. Chem. B* **2003**, *107*, 25.
(32) Yu, W. W.; Peng, X. *Angew. Chem., Int. Ed.* **2002**, *41*, 2368.
(33) Barglik-Chory, Ch.; Buchold, D.; Schmitt, M.; Kiefer, W.; Heske, C.; Kumpf, C.; Fuchs, O.; Weinhardt, L.; Stahl, A.; Umbach, E.; Lentze, M.; Geurts, J.; Müller, G. *Chem. Phys. Lett.* **2003**, *379*, 443.
(34) Chae, W. S.; Ko, J. H.; Hwang, I. W.; Kim, Y. K. *Chem. Phys. Lett.* **2002**, *365*, 49.
(35) Wu, F.; Zhang, J. Z.; Kho, R.; Mehra, R. K. *Chem. Phys. Lett.* **2000**, *330*, 237.
(36) Pardo-Yissar, V.; Katz, E.; Wasserman, J.; Willner, I. *J. Am. Chem. Soc.* **2003**, *125*, 622.
(37) Peng, Z. A.; Peng, X. *J. Am. Chem. Soc.* **2001**, *123*, 183.
(38) Katari, J. E.; Colvin, V. L.; Alivisatos, A. P. *J. Phys. Chem.* **1994**, *98*, 4109.
(39) Joswig, J. O.; Seifert, G.; Niehaus, T. A.; Springborg, M. *J. Phys. Chem. B* **2003**, *107*, 2897.
(40) Javier, A.; Yun, C. S.; Sorena, J.; Strouse, G. F. *J. Phys. Chem. B* **2003**, *107*, 435.
(41) Qu, L.; Peng, X. *J. Am. Chem. Soc.* **2002**, *124*, 2049.
(42) Peng, Z. A.; Peng, X. *J. Am. Chem. Soc.* **2002**, *124*, 3343.
(43) Wu, F.; Lewis, J. W.; Klige, D. S.; Zhang, J. Z. *J. Chem. Phys.* **2003**, *118*, 12.
(44) Brigham, E. S.; Weisbecker, C. S.; Rudzinski, W. E.; Mallouk, T. E. *Chem. Mater.* **1996**, *8*, 2121.
(45) Petrov, D. V.; Santos, B. S.; Pereira, G. A. L.; de Mello Donegá, C. *J. Phys. Chem. B* **2002**, *106*, 5325.
(46) Herz, K.; Bacher, G.; Forchel, A.; Straub, H.; Brunthaler, G.; Faschinger, W.; Bauer, G.; Vieu, C. *Phys. Rev. B* **1999**, *59*, 2888.
(47) Peranio, N.; Rosenauer, A.; Gerthsen, D.; Sorokin, S. V.; Sedova, I. V.; Ivanov, S. V. *Phys. Rev. B* **2000**, *61*, 16015.
(48) Lee, H. S.; Lee, K. H.; Choi, J. C.; Park, H. L.; Kim, T. W.; Choo, D. C. *Appl. Phys. Lett.* **2002**, *81*, 3750.
(49) Murase, N. *Chem. Phys. Lett.* **2003**, *368*, 76.
(50) Deglmann, P.; Ahlrichs, R.; Tsereteli, K. *J. Chem. Phys.* **2002**, *116*, 1585.
(51) Troparevsky, M. C.; Kronik, L.; Chelikowsky, J. R. *Phys. Rev. B* **2000**, *61*, 033311.
(52) Joswig, J.; Springborg, M.; Seifert, G.; *J. Phys. Chem. B* **2000**, *104*, 2617.
(53) Matxain, J. M.; Fowler, J. E.; Ugalde, J. M. *Phys. Rev. A* **2000**, *61*, 512.

(54) Matxain, J. M.; Fowler, J. E.; Ugalde, J. M. *Phys. Rev. A* **2000**, *62*, 553.

(55) Matxain, J. M.; Mercero, J. M.; Fowler, J. E.; Ugalde, J. M. *Phys. Rev. A* **2001**, *64*, 053201.

(56) Matxain, J. M.; Mercero, J. M.; Fowler, J. E.; Ugalde, J. M. *J. Phys. Chem. A* **2003**, *107*, 9918.

(57) Matxain, J. M.; Mercero, J. M.; Fowler, J. E.; Ugalde, J. M. *J. Am. Chem. Soc.* **2003**, *125*, 9494.

(58) Bulgakov, A. V.; Ozerov, I.; Marine, W. E-print. http://arXiv.org/abs/physics/0311117, 2003.

(59) Becke, A. D. *J. Chem. Phys.* **1993**, *98*, 5648.

(60) Hohemberg, P.; Kohn, W. *Phys. Rev.* **1964**, *136*, 3864.

(61) Lee, C.; Yang, W.; Parr, R. G. *Phys. Rev. B* **1988**, *37*, 785.

(62) Becke, A. D. *Phys. Rev. A* **1988**, *38*, 3098.

(63) Stevens, W. J.; Krauss, M.; Basch, H.; Jasien, P. G. *Can. J. Chem.* **1992**, *70*, 612.

(64) Schmidt, M. W.; Baldridge, K. K.; Boatz, J. A.; Elbert, S. T.; Gordon, M. S.; Jensen, J. H.; Koseki, S.; Matsunaga, N.; Nguyen, K. A.; Su, S. J.; Windus, T. L.; Dupuis, M.; Montgomery, J. A. *J. Comput. Chem.* **1993**, *14*, 1347−1363 (*GAMESS*).

(65) Frisch, M. J.; Trucks, G. W.; Schlegel, H. B.; Scuseria, G. E.; Robb, M. A.; Cheeseman, J. R.; Zakrzewski, V. G.; Montgomery, J. A., Jr.; Stratmann, R. E.; Burant, J. C.; Dapprich, S.; Millam, J. M.; Daniels, A. D.; Kudin, K. N.; Strain, M. C.; Farkas, O.; Tomasi, J.; Barone, V.; Cossi, M.; Cammi, R.; Mennucci, B.; Pomelli, C.; Adamo, C.; Clifford, S.; Ochterski, J.; Petersson, G. A.; Ayala, P. Y.; Cui, Q.; Morokuma, K.; Malick, D. K.; Rabuck, A. D.; Raghavachari, K.; Foresman, J. B.; Cioslowski, J.; Ortiz, J. V.; Stefanov, B. B.; Liu, G.; Liashenko, A.; Piskorz, P.; Komaromi, I.; Gomperts, R.; Martin, R. L.; Fox, D. J.; Keith, T.; Al-Laham, M. A.; Peng, C. Y.; Nanayakkara, A.; Gonzalez, C.; Challacombe, M.; Gill, P. M. W.; Johnson, B. G.; Chen, W.; Wong, M. W.; Andres, J. L.; Head-Gordon, M.; Replogle, E. S.; Pople, J. A. *Gaussian 98*, revision A.7; Gaussian, Inc.: Pittsburgh, PA, 1998.

(66) Jortner, J. *Z. Phys. D: At., Mol. Clusters* **1992**, *24*, 247.

(67) Hartke, B. *Angew. Chem., Int. Ed.* **2002**, *41*, 1468−1487 and references therein.

(68) Lide, D. R., Ed. *Handbook of Chemistry and Physics*, 79th ed.; CRC Press: Boca Raton, FL, 1998−1999; pp 5−24.

(69) Knight, W. D.; Clemenger, K.; de Heer, W. A.; Saunders, W. A.; Chou, M. Y.; Cohen, M. L. *Phys. Rev. Lett.* **1984**, *52*, 2141.

(70) Clemenger, K. *Phys. Rev. B* **1984**, *32*, 1359.

(71) Raty, J. Y.; Galli, G.; Bostedt, C.; van Buuren, T. W.; Terminello, L. J. *Phys. Rev. Lett.* **2003**, *90*, 7401.